

We E102 06

3D Inverse Scattering Series Method for Internal Multiple Attenuation

M. Wang* (CGG) & B. Hung (CGG)

SUMMARY

In this paper, we show the first application of the 3D inverse scattering series (ISS) method for internal multiple attenuation. The ISS method is a data-driven approach that can predict all internal multiples without any prior knowledge of subsurface information. We discuss the implementation of the true-azimuth 3D ISS based method which is suitable for conventional streamer data. We apply the approach on a synthetic example as well as data acquired from the Santos Basin, offshore Brazil. The results show that the 3D prediction and subtraction method outperforms the 2D method as it takes into account out-of-plane multiple contributions.

Introduction

Internal multiple attenuation has received increasing attention in recent years because of the demand for accurate imaging and interpretation. This kind of multiple is generated by a series of subsurface impedance contrasts such as coal seams and geological unconformities. Internal multiples are commonly observed in seismic data, for example, in the Santos Basin of Brazil, whereby the multiples generated between the seafloor and the salt structures have similar traveltimes with the reflections from the pre-salt reservoir. This poses significant problems for reservoir identification and characterization.

Removal of internal multiples is a long-standing problem and is still very challenging for the industry. Several methods were developed to address this problem such as Delft's feedback model (Berkhout and Verschuur, 1997), Jakubowicz's convolution-correlation method (Jakubowicz, 1998), model driven methods (Pica and Delmas, 2008) and the inverse scattering series (ISS) based method (Weglein *et al.* 1997). The first three methods require some form of subsurface information such as the multiple-generating horizons or seismic velocity for predicting the internal multiples. When more multiple-generating horizons are present in the data, iterative modelling is often required to attenuate all the multiples. In certain geologic settings, multiple generators can exist laterally for thousands of meters and picking horizons is a challenging task (assuming they can be identified in the first place), especially for a complex 3D survey. In contrast, the ISS based method is a data-driven approach that can predict all internal multiples simultaneously without any knowledge of subsurface information. Hence, ISS can be an effective tool for internal multiple suppression.

We have implemented 2D ISS and successfully applied it on field data for attenuating internal multiples (Wang *et al.* 2012). However, 2D ISS is ineffective for data from the Santos Basin due to the highly undulating salt structures, which generate multiples with a strong out-of-plane component. Extending the method from 2D to 3D is straightforward in theory, but the lack of data in the crossline direction has made 3D ISS prediction very difficult for conventional streamer data. We overcome this difficulty by constructing high density and wide azimuth data from the existing streamer geometry, the same approach that was used in 3D SRME (Lin *et al.*, 2004) and 3D internal multiple attenuation (Hung *et al.*, 2013). In this paper, we discuss the implementation of 3D ISS internal multiple attenuation and apply the method on a synthetic and real seismic dataset. Both examples show that the 3D method offers an improved result compared to the 2D method. To the best of our knowledge, this is the first application of the 3D ISS based method on field data for internal multiple attenuation.

Method

The ISS based method assumes that the input data is free of coherent noise such as source and receiver ghost events, direct waves and surface-related multiples. As shown in Equation (1), internal multiple D_{IM} is predicted by selecting parts of the odd inverse subseries which is associated with removing multiply-reflected energy (Weglein *et al.*, 1997),

$$D_{IM}(k_g, k_s, \omega) = (-2iq_s)^{-1} \sum_{n=1}^{\infty} b_{2n+1}(k_g, k_s, q_g + q_s) \quad (1)$$

where q is the vertical wavenumber, k is the horizontal wavenumber (including two components along the x and y direction for the 3D case). The wavenumber q and k satisfy the relationship of $k_x^2 + k_y^2 + q^2 = (\omega/c_0)^2$, where ω is the angular temporal frequency, and c_0 is the reference velocity (water velocity for marine surveys). Subscripts g and s stand for geophone/hydrophone and source respectively. The first attenuator b_3 is used for attenuating the first order internal multiple. It is a 5D data volume for the 3D case, which is shown in Equation (2),

$$\begin{aligned} b_3(k_{gx}, k_{gy}, k_{sx}, k_{sy}, q_g + q_s) \\ = \int_{-\infty}^{\infty} \int_{-\infty}^{\infty} e^{-iq_1(z_g - z_s)} dk_{1x} dk_{1y} \int_{-\infty}^{\infty} \int_{-\infty}^{\infty} e^{iq_2(z_g - z_s)} dk_{2x} dk_{2y} \times \int_{-\infty}^{\infty} e^{i(q_g + q_s)z_1} b_1(k_{gx}, k_{gy}, k_{1x}, k_{1y}, z_1) dz_1 \\ \times \int_{-\infty}^{z_1 + \epsilon} e^{-i(q_1 + q_2)z_2} b_1(k_{1x}, k_{1y}, k_{2x}, k_{2y}, z_2) dz_2 \times \int_{z_2 + \epsilon}^{\infty} e^{i(q_2 + q_s)z_3} b_1(k_{2x}, k_{2y}, k_{sx}, k_{sy}, z_3) dz_3 \end{aligned} \quad (2)$$

where $b_1(k_{gx}, k_{gy}, k_{sx}, k_{sy}, z)$ is the pseudo-migrated data using the reference velocity from $b_1(k_{gx}, k_{gy}, k_{sx}, k_{sy}, q_s + q_g)$, which is defined in terms of input data D in the frequency domain by Equation (3).

$$b_1(k_{gx}, k_{gy}, k_{sx}, k_{sy}, q_g + q_s) = -2iq_s D(k_{gx}, k_{gy}, k_{sx}, k_{sy}, \omega) \quad (3)$$

z is a variable in pseudo depth, z_s and z_g are source and receiver depths, respectively and ε is a positive quantity to ensure that z_1 and z_3 are always greater than z_2 . In practice, ε is slightly longer than source wavelet length. Higher-order attenuators b_n ($n = 5, 7 \dots \infty$), can be formulated in a similar way that satisfy the “low-high-low” relationship (Nita and Weglein, 2007) for internal multiple prediction. The first attenuator b_3 can predict the first order internal multiple with correct travel-time and less accurate amplitude. Including higher-order attenuators in the prediction can enhance the amplitude accuracy but at the expense of longer computational time. Therefore, our strategy is to use only the first attenuator b_3 in the prediction and then rely on adaptive subtraction to handle the amplitude difference between the actual internal multiple and the predicted ones.

True-azimuth 3D implementation

3D ISS internal multiple prediction requires an ideal data distribution, e.g. a dense distribution of sources and receivers at coincident positions in a grid-like acquisition. Due to the high cost of acquiring such data, we replicate this acquisition using an approach that was employed on conventional streamer data for 3D SRME (Lin *et al.*, 2004) and 3D internal multiple prediction (Hung *et al.*, 2013). This technique allows for true-azimuth 3D ISS internal multiple attenuation. The approach is as follows: (1) generate a regularized wide azimuth data by choosing the appropriate traces from input (depending on some selection criteria that minimize the difference in azimuth, offset and midpoint) and then applying differential NMO to correct the discrepancy in offset; (2) perform 3D ISS for internal multiple prediction on the regularized data; then (3) map the internal multiple model to the irregular locations; and finally (4) apply adaptive subtraction schemes to remove the internal multiples from the input data.

Synthetic and Field Data Examples

The 3D ISS based method was first validated with a synthetic dataset. A 3D synthetic dataset was generated by acoustic wave-equation modelling using the velocity function shown in Figure 1a. All the primary events are the generators of the internal multiples and the shallowest two events have significant dip in the crossline direction, as shown in Figure 1b. Without identifying the multiple-generating interfaces, all the internal multiples are predicted by the 3D and 2D ISS method. We compare the results from an outer cable which has 200 meters inline distance from the shot line. Figure 2a show a near-offset section of input data. The blue-dashed lines indicate the exact traveltimes of two strong internal multiples. As a reference, the 2D model is shown in Figure 2b. The 3D ISS multiple model is depicted in Figure 2c. The wiggle displays are the magnified sections (dashed-red box) that highlight the extent of matching between the input (coloured wiggle) and the predicted multiples (grey wiggle). It can be seen that the 3D model exhibits superior matching in the traveltimes compared with the input than the 2D model. This is because the 2D method does not take into account the out-of-plane reflections that contribute to the generation of the internal multiples. Consequently, it puts more constraints on the subsequent process of adaptive subtraction. Figure 3a is the same input data as Figure 2a. There is much more residual of the internal multiples left in the 2D output, especially at the locations indicated by arrows in Figure 3b. In comparison, all the internal multiples are attenuated while primaries are well preserved in the 3D output shown in Figure 3c.

The effectiveness of the ISS method can be further illustrated using a field data example. Internal multiples are a particular problem in the Santos Basin, Brazil. If not suppressed, their presence affects the quality of the final seismic image. A series of impedance contrasts above the pre-salt reservoir can be observed such as the water bottom (WB), top of salt (TOS) and the layered salt structures as shown in Figure 4a. All these reflectors generate internal multiples which interfere with the reflections from the reservoir. Figure 4b is the crossline view from one location which is indicated by the blue line in Figure 4a. It can be observed that the salt structures have significant crossline dip which introduces a strong 3D effect to the generation of the internal multiples. Consider the subsalt area which is highlighted by the green box in Figure 4a. The near-offset stack sections of input, ISS subtraction results and their differences are depicted in Figure 5. In this section, the predicted multiples are

mainly generated between the seafloor and top of salt as well as from the top of salt and layered evaporites. They are relatively weaker than the primaries, but still can be observed and attenuated from input data. Compared with the 2D results, the improvement from the 3D approach is evident. The predicted 3D multiple models are more continuous leading to a better multiple attenuation and primary preservation as shown in Figure 5c and 5e.

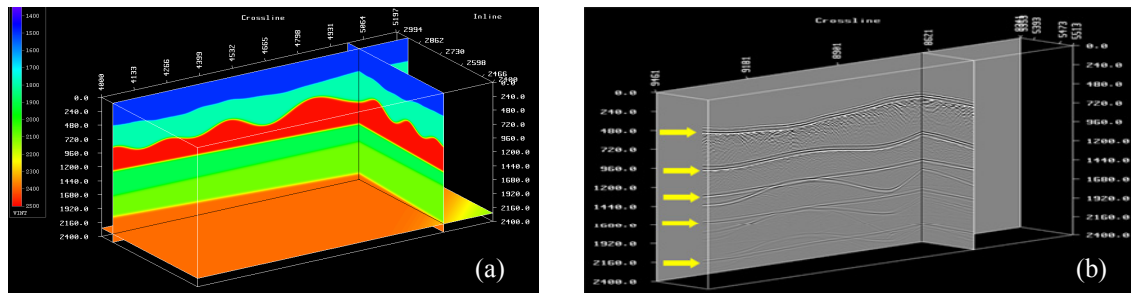


Figure 1 (a) 3D velocity profile for generating the synthetic data. (b) A portion of 3D offset cube with the five primary events highlighted by the arrows.

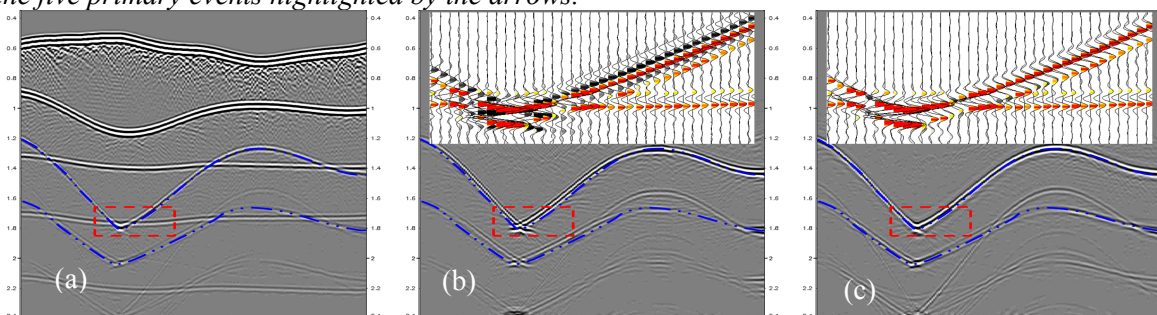


Figure 2 Near-offset section for (a) Input, (b) 2D ISS model, and (c) 3D ISS model. The blue-dashed lines indicate two strong internal multiples, which are drawn from the input section. The wiggle displays show the overlay between the input and the model.

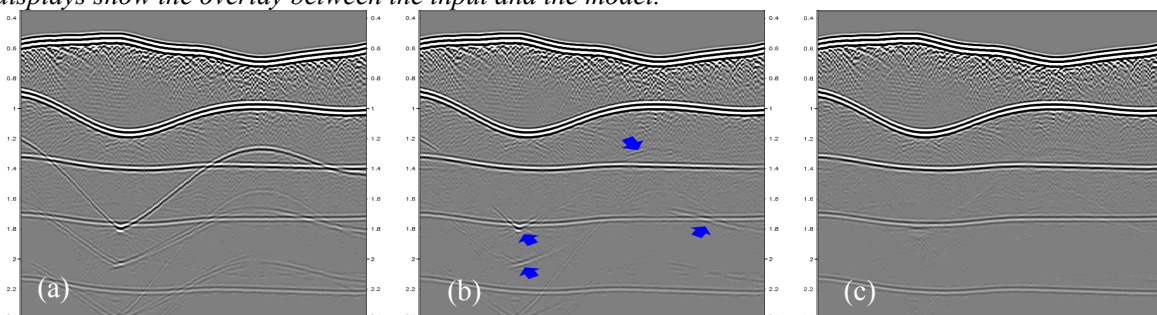


Figure 3 Near-offset section for (a) Input, (b) 2D output, and (c) 3D output. Blue arrows indicate the residual internal multiples left in 2D case.

Conclusions

We have discussed the implementation of a true-azimuth 3D inverse scattering series method (ISS) for internal multiple attenuation. This method can predict internal multiples produced from all possible generators simultaneously, without requiring any subsurface information. We first apply the method on a synthetic example and then show results from a field dataset acquired in the Santos Basin, offshore Brazil. 3D ISS is more effective than the 2D approach since it takes into account the strong crossline dip of multiple generators. This is the first 3D field example using ISS method for internal multiple attenuation.

Acknowledgments

The authors would like to thank CGG for permission to publish this work. Appreciation is given to Dechun Lin and Kunlun Yang for their helpful discussions and to Chu-Ong Ting and Nicolas Chazalnoel for the preparation of the input dataset.

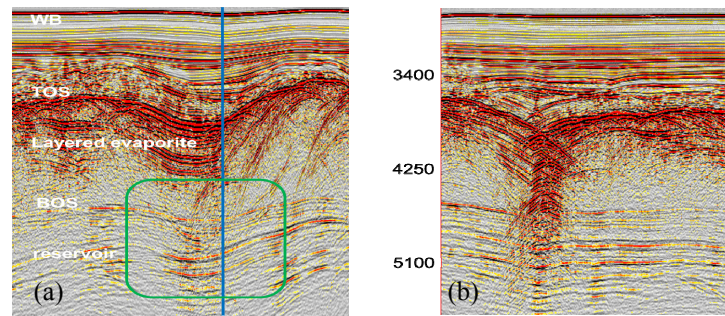


Figure 4 (a) Common-offset section from Santos Basin, Brazil which include strong reflections such as water bottom (WB), top of salt (TOS), bottom of salt (BOS) and layered salt structures. (b) crossline view from the location indicated by blue line in (a), which show strong crossline dip of salt structures.

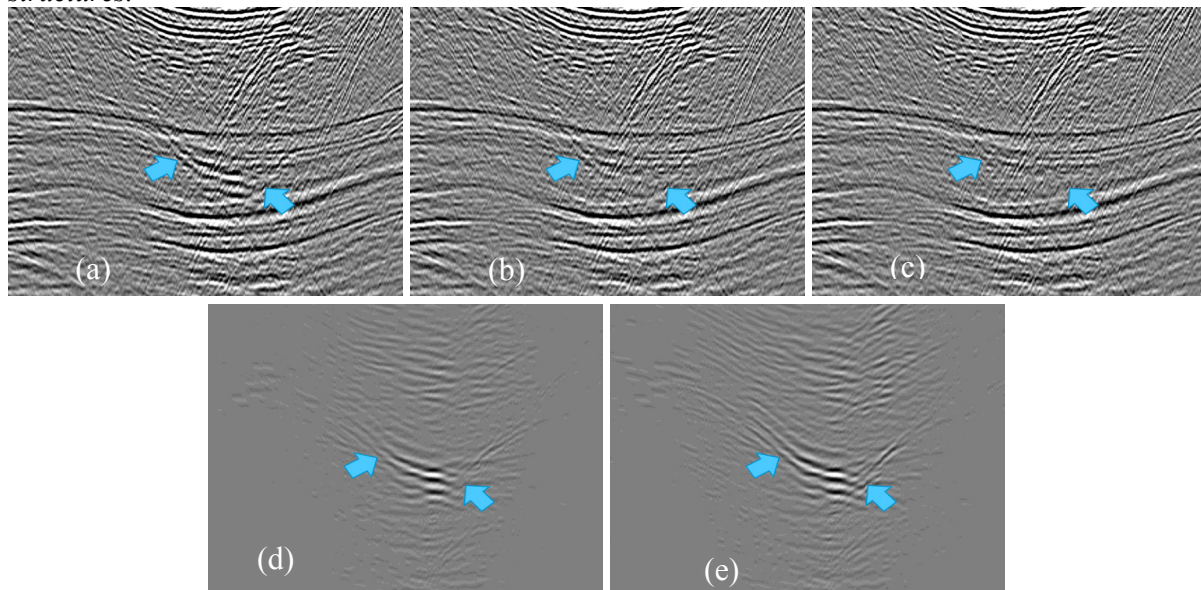


Figure 5 Near-offset stack sections of zoomed area (green box in Figure 4a). (a) Input, (b) 2D ISS output, (c) 3D ISS output, (d) 2D ISS difference, and (e) 3D ISS difference. Blue arrow indicates residual internal multiples left in 2D output, and better results in the 3D case.

References

- Berkhout, A.J. and Verschuur, D.J. [1997] Estimation of multiple scattering by iterative inversion, Part I: Theoretical considerations. *Geophysics*, **62**, 1586-1595.
- Hung, B., Wang, M. and Griffiths, M. [2013] True-azimuth 3D internal multiple attenuation without subsurface information. *75th Meeting, EAGE*, Expanded Abstracts, Tu 14 02.
- Jakubowicz, H. [1998] Wave equation prediction and removal of interbed multiples. *68th Meeting, SEG*, Expanded Abstracts, 1527-1530.
- Lin, D., Young, J., Huang, Y. and Hartmann, M. [2004] 3D SRME Applications in Gulf of Mexico. *74th Internat. Mtg., Soc. Expl. Geophys.*, Expanded Abstracts, 1257-1260.
- Nita, B.G. and Weglein, A.B. [2007] Inverse scattering internal multiple attenuation algorithm: an analysis of the pseudo-depth and time monotonicity requirements. *77th Meeting, SEG*, Expanded Abstracts, 2461-2464.
- Pica, A. and Delmas, L. [2008] Wave equation based internal multiple modelling in 3D. *78th Meeting, SEG*, Expanded Abstracts, 2476-2480.
- Wang, M., Hung, B. and Xin, K. [2012] Application of inverse scattering series method for internal multiple attenuation – A case study. *22nd Meeting, ASEG*, Expanded Abstracts, Vol. 2012 No.1.
- Weglein, A.B., Gasparotto, F.A., Carvalho, P.M. and Stolt, R.H. [1997] An inverse-scattering series method for attenuating multiples in seismic reflection data. *Geophysics*, **62**, 1975-1989.